

Long-term decoding of arm movement using Spatial Distribution of Neural Patterns

Vijay Aditya Tadipatri[†], Ahmed H. Tewfik[†], James Ashe^{*}

Abstract—Day to day variability and non-stationarity caused by changes in subject motivation, learning and behavior pose a challenge in using local field potentials (LFP) for practical Brain Computer Interfaces. Pattern recognition algorithms require that the features possess little to no variation from the training to test data. As such models developed on one day fail to represent the characteristics on the other day. This paper provides a solution in the form of adaptive spatial features. We propose an algorithm to capture the local spatial variability of LFP patterns and provide accurate long-term decoding. This algorithm achieved more than 95% decoding of eight movement directions two weeks after its initial training.

Index Terms—Local Field Potentials, Long-term decoding, Brain Computer Interface.

I. INTRODUCTION

Signals recorded from the brain can decode various motor behaviors in terms of arm position and velocity. Such decoders can help in building neural prosthetic to aid patients suffering from paraplegia [1]. For practical applications, a neural prosthetic requires a high quality signal and an extraction modality that can provide long-term signal acquisitions. Intracortical recordings like Single Unit Activity (SUA) and Local Field Potentials (LFP) have high SNR and better spatial resolution than non-invasive modalities, making them a good choice for neural prosthetic applications [2]. Recent advances in neural engineering also show evidence of long-term acquisition; for example, SUA was recorded over 300 - 500 days in monkeys [3], [4] and over 1000 days in a paraplegic patient [5]. However, one of the challenges plaguing these modalities is the day-to-day variation of the recorded signal characteristics due to changes in subject motivation, behavior, and training [6]. Such variations pose a challenge to current pattern recognition tools that expect little or no changes to signal characteristics between training and testing data set. To counter this problem, several solutions have been proposed. Although building day specific decoders is a popular strategy, it ignores the variation of neural patterns and needs daily calibration of the decoder that can encumber the BCI user [7]. Other papers propose the use of a static decoder and push the training burden on the user [8]. This strategy has shown to be effective in closed-loop where visual feedback can be leveraged. Also, an adaptive decoder that learns new neural patterns provided stable decoding over multiple recording days [9].

A successful adaptation strategy requires a good understanding of the neural pattern variability. To this end, researchers have hypothesized a reorganization of the firing patterns in different areas of the brain [10]. McKenzie et al. found that patterns from novel behaviors diverged from the patterns associated with pre-learning behaviors. While, some studies provide evidence of motor adaptation to changes in external environments, the changes in the brain due to this adaptation is not completely understood [11], [12]. The main objective of this paper is to characterize the neural patterns in terms of their spatial patterns and their distributions. We hypothesize that the observed neural patterns are sampled from a spatial distribution and estimating this distribution aids in long-term decoding. neural patterns neural plasticity can be characterized. For this purpose we devised an algorithm to predict arm movements to 8 different directions and evaluated its performance when neural spatial variability is considered. We present the stability of such decoders developed for multi-channel LFP over multiple recording sessions in two monkeys when they were performing a center-out reach task. This paper investigates the effect of spatial variability on the accuracy of the model (trained on a single session) to decode eight directions of arm movement and its consistency over multiple weeks.

To decode the eight directions of movement, the proposed algorithm estimates the trajectory of arm movement and decodes the target direction by measuring the angle of the estimated trajectory. The arm trajectory is estimated with the use of redundant non-linear regressors in the form of relevance vector machine (RVM) [13] as follows: $t(X) = \mathbf{w}^T \Phi(X)$, where y is the arm position for a corresponding neural feature input vector X and an appropriate kernel function $\Phi(\cdot)$. RVM produces a good fit for the trajectory by using a sparse formulation and derives that the weights \mathbf{w} from a zero mean Gaussian distribution [13]. We observed if each of the x,y position were modeled independently, correlations in these results in spurious estimates, i.e., good estimates in one component do not translate to other. We propose to use a kernel dependency estimate framework to simultaneously estimate both components [14] as discussed in II-B. The proposed algorithm outperforms the state-of-the-art classifiers providing > 81% decoding over two weeks.

The rest of this paper is organized in the following way: Section II discusses the method used to characterize neural patterns; Section III provides information on the neural and behavioral data; Section IV discusses the results of the hypothesis in terms of decoding accuracy and; Section V provides some concluding remarks.

[†]V.A.Tadipatri and A.H.Tewfik are with The Dept. of Electrical and Computer Engineering, The University of Texas, Austin, TX

^{*}J.Ashe is with The Dept. of Neuroscience, University of Minnesota, Minneapolis MN

II. METHODS

This section discusses the modeling technique used to analyze the spatial patterns in data and to obtain stable decoders. Section II-C discusses the formulation of such neural patterns. In BCI faithful decoding of arm movement requires the model to estimate multiple kinetic parameters. Section II-B discusses the proposed solution to simultaneously estimate multiple parameters. To estimate these parameters from the neural features, a regression model in the form of RVM is used II-A. Lastly, we discuss the use of adaptation to obtain stable decoding over multiple recording sessions.

A. Relevance Vector Machine

RVM is a set of general models in the form of equation 1

$$t(\mathbf{X}) = \sum w_i \Phi(\mathbf{X}, \mathbf{Y}_i) + w_0 \quad (1)$$

where \mathbf{Y}_i are the different basis vectors and $\Phi()$ is the kernel function that measures the similarity between input neural feature vector \mathbf{X} and the basis vectors. This approach generalizes well while having a sparse support in the form of few non-zero w_i [13]. The relevant vectors (support vectors) chosen by RVM are significantly different from SVM. SVM gathers vectors closer to the decision boundary which growing the number of support vectors linearly with the training set. In contrast, RVM gathers prototypical examples from the training data that lie at the center of the training set [13]. Please refer to [13] for more details on the RVM framework.

B. Multiple output regression

In this paper, the arm direction is decoded by estimating the arm position and then calculating the target direction as the $\arctan\{y/x\}$ of the horizontal x and vertical y components or the arm position. This method also allows generalization to novel targets and external fields. The regular RVM is formulated to provide a sparse solution for a single output and here we present an approach to estimate multiple output components simultaneously. The naive approach constructs separate regression models for each individual components. While this results in good estimates of individual components, the overall trajectory suffers as the individual regressions do not account for correlations between the horizontal and vertical components of arm movement. Kernel Dependency Estimation (KDE) allows to leverage this observation [14]. The chosen output kernel Ψ reflects the non-linear dependency of output variables and build a suitable model for each basis element of the kernel. Here we use the following Gaussian kernel:

$$\Psi(\mathbf{y}, \mathbf{y}_i) = \exp(-(\mathbf{y} - \mathbf{y}_i) \Sigma_y^{-1} (\mathbf{y} - \mathbf{y}_i)^T) \quad (2)$$

where \mathbf{y}_i are points sampled from a circular grid of radius 10cm., and Σ_y is spread of the basis vector. The dimensionality of this kernel can be reduced by choosing to represent only the highest energy components of the kernel.

$$\Psi = USV^T \quad (3)$$

$$U_b = \sum w_{bi} \Phi(X) + w_{b0}$$

Algorithm 1 Learning and Adapting Movement Decoder

Initial Model Learning Obtain Model from Neural Features and Targets: \mathcal{M} from $\{\mathbf{X}_i, \mathbf{t}_i\}_{i=1}^N$

Build Input Kernel : $\Phi(\mathbf{X}_i, \mathbf{X}_i)$ using eq (4)

Build Output Kernel : $\Psi(\mathbf{t}_i, \mathbf{y}_j)$ using eq (2)

$\Psi = USV^T$

for each column k of U **do**

Estimate $\mathbf{w}_k : U_k = \sum_{i=1}^N w_{ki} \Phi(X) + w_{k0}$

$\mathbf{w}_k : \min \|U_k - \sum_{i=1}^N w_{ki} \Phi(X) + w_{k0}\|_2 + \lambda |\mathbf{w}_k|_0$

end for

Basis Vectors : $\mathbf{D} \leftarrow \mathbf{X}$

Store Model: $\mathcal{M}_0 \leftarrow \{S, V, \mathbf{D}, \mathbf{w}\}$

Initialize $\mathcal{M}^* \leftarrow \mathcal{M}_0$

Model Evaluation: Estimate Targets from Neural Features: $\hat{\mathbf{t}}_i$ from $\{\mathbf{X}_i^*\}_{i=1}^N$

Build Input Kernel : $\Phi(\mathbf{X}_i^*, \mathbf{D}_j)$ using eq (4)

for each column k of U **do**

Calculate $\hat{U}_k = \sum_{j=1}^{ND} w_{kj} \Phi_j(X) + w_{k0}$

end for

$\hat{\Psi} = \hat{U} S V^T$

$\hat{\mathbf{t}}_i = \max_i \hat{\Psi}_i, \hat{\theta}_i = \arctan \frac{t_y}{t_x}$

Model Adaptation: Update Model after L trials: \mathcal{M}^* from $\{\mathbf{X}_i^*, \hat{\theta}_i^*\}_{i=1}^L, \mathcal{M}$

$\tilde{\mathbf{t}} = \mathcal{F}(\hat{\theta}_i)$

$\tilde{\Psi} = \Psi(\tilde{\mathbf{t}}_i, \mathbf{y}_j)$ using eq (2)

$\tilde{U} = \tilde{\Psi} V S^{-1}$

for each column k of U **do**

Update $\mathbf{w}_k^u : \tilde{U}_k - \hat{U}_k = \sum_{i=1}^N w_{ki}^u \Phi(\mathbf{X}_i^*) + w_{k0}^u$

end for

Basis Vectors : $\mathbf{D}^u \leftarrow \mathbf{X}^*$

$\mathcal{M}^* \leftarrow \{S, V, \mathbf{D} | \mathbf{D}^u, \mathbf{w} | \mathbf{w}^u\}$

One of the challenges for KDE is the pre-image identification that refers to identifying the correct basis given the value of the kernel [14]. We adopt a maximum likelihood approach by identifying the target basis that provides the maximum kernel value.

C. Spatial Distributions in Neural Patterns

The above algorithm using RVM considers a neural feature vector and ignores any spatial information between the features. We hypothesize that some of the day to day variability is due to a spatial shift in the neural patterns and by modeling the spatial shift, we obtain a better decoder. While a spatial laplacian filter has been proposed for a similar purpose, it merely smooths the whole vector and some details are lost. The ideal solution should process not only a predefined spatial filter but also any arbitrary pattern. For this purpose, we introduce a new kernel that measures the similarity at all the neighboring locations of the feature vectors. Consider

two neural feature vectors \mathbf{X}, \mathbf{Y} measured at N locations.

$$\Phi(\mathbf{X}, \mathbf{Y}, \sigma_s) = \prod_{n=1}^N \frac{1}{|K|} \sum_{k \in K} z(k, n) \exp\left(-\frac{(x_k - y_n)^2}{\sigma^2}\right) \quad (4)$$

$$z(k, n) = \begin{cases} \exp\left(-\frac{(k-n)^2}{\sigma_s^2}\right), & \text{Gaussian} \\ 1, & \text{Uniform} \end{cases} \quad (5)$$

where, K is the set of all neighboring locations of recording location n . The value σ_s in equation (5) modulates the spatial distribution and σ captures the variation in the magnitude at the electrode location. The equation (4) calculates a distance metric similar to a radial basis function (RBF). However, the presented formulation also calculates the similarity between the neighboring locations along with the current electrode location and weighs the similarity with a spatial gaussian. In this work only locations that are σ_s distance away are considered as neighbors. The regular RBF kernel is a special variant of this basis and can be obtained by setting σ_s to 0.

D. Decoder Adaptation over time

The model decodes estimates of arm position for a new test neural vector, \mathbf{X}_{new} , as

$$\hat{y}_{new} = \sum \mathbf{w}_b^T \Phi(\mathbf{X}_{new}, \mathbf{X}_b)$$

In an ideal situation, where all possible neural representations are available, this model can provide good generalization. However, neural vectors tend to deviate from the model parameters. While the spatial variability of the patterns captures some of this deviation, it is advantageous if the decoder can adapt to these novel patterns. Since intended hand movements are unavailable to the neural decoder, we assume that the monkey intends to reach the target in a straight line. Thus, we approximate the intended trajectory as $\tilde{y} = \mathcal{F}(\hat{\theta})$ as shown in Figure 1. This approach eliminates the need for a daily calibration session and can perform online updates without interrupting the user. Algorithm 1 provides a pseudo code for learning and adapting movement decoders. The initial learning stage is executed on calibration data obtained from the BCI user. This model is then evaluated on subsequent neural data to provide hand movements. Since, the neural patterns evolve over different days, the model needs to be updated after $L(25)$ trials. The next section describes the LFP data used to validate our hypothesis.

III. DATA

Two male rhesus monkey subjects (*Macaca mulatta*), H564 and H464, both left armed, were trained in an instructed-delay center-out task using a manipulandum. Two silicon-based electrode arrays (Cyberkinetics, Foxboro, MA) were implanted in the contra-lateral arm areas of primary motor (M1) and dorsal premotor (PMd) cortices respectively. Under all task conditions the subject executed two-dimensional horizontal reaching movements with the manipulandum from a central location to one of eight targets equally spaced around a circle of radius 9cm. The target locations were randomized within sets of eight and the subject had to

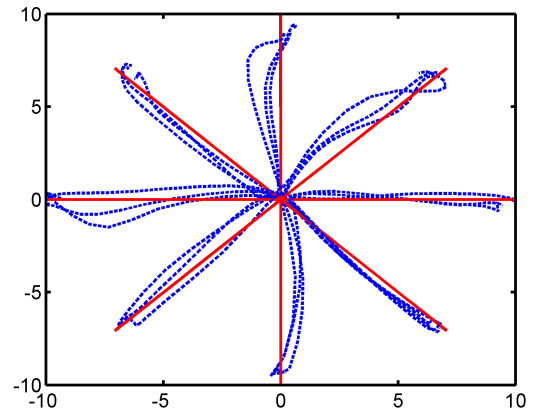


Fig. 1. Actual (\hat{t} , dashed blue), and the used intended movement (\tilde{t} , solid red) of example trials overlaid on a 10cm \times 10cm workspace.

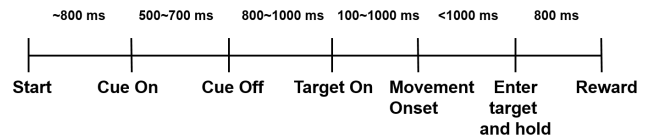


Fig. 2. Time line of a single trial with a median time spent during each stage of the trials.

complete correct movements in all eight directions before moving onto the next set. Figure 2 shows the time line for each trial with a median time spent at each stage of the trial. Only those trials that were performed correctly were stored for further analysis. LFP data were filtered between 0.3Hz and 220Hz, and sampled at 1KHz. We preprocessed the data to prune out any noisy recordings from the analysis. We trained models on the data collected in session 1 (recorded on day 1), and tested its performance on the subsequent sessions. During our initial analysis, we observed that band-pass filtering the signal in the δ - band (0.4 - 4Hz) obtained the best decoding result. Hence, we calculate qualitative features in the form of instantaneous inter-channel power ranks on the data filtered in this band [15].

IV. RESULTS AND DISCUSSION

To understand the effects of changes in neural patterns, we train a model on data collected on day 1 of the recordings and evaluate its performance on the data from subsequent days. We use the decoding accuracy obtained from the models to compare results from two approaches. Decoding accuracy is defined as the ratio of number of trials where movement direction was correctly decoded to the total number of trials in the session. Note that the monkeys perform the tasks in an open loop and do not receive any feedback from the decoder performance.

We hypothesize that learning modulates the neural patterns and tends to change them from an initial pattern. In this paper we investigate if the changes to the neural pattern are local or if they are very different from the initial pattern. To

TABLE I
DECODING ACCURACY (IN %) OVER DECODER AGE.

Decoder Age	8	9	13	14
H464				
No Spatial Shift	92	88	80	66
Spatial Shift	91	88	77	81
Daily Adaptation				
No spatial Shift	98	97	96	97
Spatial Shift	94	92	87	82
H564				
No Spatial Shift	74	61		
Spatial Shift	75	59		
Daily Adaptation				
No spatial Shift	80	66		
Spatial Shift	81	63		

understand the effect of spatial shift we varied the value of σ_s and monitored the decoding performance. Also, in this paper we shall assume that a shift in pattern has occurred at all locations. To obtain a fair comparison, all the other settings for the experiments were kept constant.

We first compare the results from varying the spatial shift in the algorithm. For this analysis, decoder was not adapted. The results are presented in the first few rows of Table I. We can observe that a decoder that accounts for the spatial variation provides performs similarly to a decoder that does not. However, in the later sessions it provides much higher performance. These results show that while considering spatial shifts in the neural patterns might not aid in the short-term performance of a neural decoder, it definitely assists in the long-term. We observed that after two weeks a non-adaptive decoder could accurately decode 80% (in comparison to 66%) of arm movements. Even in the short-term these decoders have comparable performance.

Similarly results from decoders that adapted over testing trials is also presented. The decoder adaptation is done by appending the newly obtained neural features after 25 trials and retraining the decoder. During adaptation, the decoder gradually learns the new patterns by reinforcing the patterns. Hence, it is expected that the performance with adaptation is better than without. As observed from the Table 1, effect of adaptation dominates the subtle variations in spatial neural patterns and provides stable decoding. Also, we see that adapting on the spatial shift data is not efficient and provides slightly less performance. This is because there is very little spatial shift of the neural patterns during a single recording session. Also, while the accuracy of the decoder is slightly low, it uses significantly less number of basis to obtain a comparable result.

V. CONCLUSION

In this paper, we tested the hypothesis that neural patterns change locally during repeated execution of the same behavior. Based on this hypothesis we developed a new kernel function to incorporate local spatial variations of neural patterns. Decoders based on these new kernels provided comparable decoding in the short-term and significantly better decoding in the long-term. These results indicate

that considering local changes to the neural patterns might aid in building practical neural prosthetic devices. Finally, we show that by adapting to the day to day variations of the patterns achieves significantly higher decoding. Using such an adaptive decoder achieves $> 95\%$ decoding over two weeks of recording. In this paper, we assume that changes local to all electrodes occur over time. It is indeed possible that only a subset of these electrodes show such characteristics. Future work will address the subset selection of electrodes.

REFERENCES

- [1] Leigh R. Hochberg, Mijail D. Serruya, Gerhard M. Friehs, Jon A. Mukand, Maryam Saleh, Abraham H. Caplan, Almut Branner, David Chen, Richard D. Penn, and John P. Donoghue, "Neuronal ensemble control of prosthetic devices by a human with tetraplegia," *Nature*, vol. 442, no. 7099, pp. 164–171, July 2006.
- [2] AP Georgopoulos, AB Schwartz, and RE Kettner, "Neuronal population coding of movement direction," *Science*, vol. 233, pp. 1416–1419, 1986.
- [3] Adam S. Dickey, Aaron Suminski, Yali Amit, and Nicholas G. Hatsopoulos, "Single-unit stability using chronically implanted multi-electrode arrays," *Journal of Neurophysiology*, vol. 102, no. 2, pp. 1331–1339, Aug. 2009, PMID: 19535480 PMID: PMC2724357.
- [4] S. Suner, M.R. Fellows, C. Vargas-Irwin, G.K. Nakata, and J.P. Donoghue, "Reliability of signals from a chronically implanted, silicon-based electrode array in non-human primate primary motor cortex," *IEEE Transactions on Neural Systems and Rehabilitation Engineering*, vol. 13, no. 4, pp. 524–541, 2005.
- [5] J. D. Simeral, S.-P. Kim, M. J. Black, J. P. Donoghue, and L. R. Hochberg, "Neural control of cursor trajectory and click by a human with tetraplegia 1000 days after implant of an intracortical microelectrode array," *Journal of Neural Engineering*, vol. 8, no. 2, pp. 025027, Apr. 2011.
- [6] W Jensen and P.J. Rousche, "On variability and use of rat primary motor cortex responses in behavioral task discrimination," *Journal of Neuro Engineering*, vol. 3, pp. L7–L13, 2006.
- [7] Joaquin Q. Candela, Masashi Sugiyama, Anton Schwaighofer, and Neil D. Lawrence, *Dataset Shift in Machine Learning*, The MIT Press, 2009.
- [8] Karunesh Ganguly and Jose M. Carmena, "Emergence of a stable cortical map for neuroprosthetic control," in *Article ID e1000153*, 2009.
- [9] Vijay Aditya Tadipatri, Ahmed Tewfik, and James Ashe, "Long-term movement tracking from local field potentials with an adaptive open-loop decoder," in *ICASSP2014 - Bio Imaging and Signal Processing (ICASSP2014 - BISP)*, Florence, Italy, May 2014, pp. 5911–5915.
- [10] Sam McKenzie, Nick T. M. Robinson, Lauren Herrera, Jordana C. Churchill, and Howard Eichenbaum, "Learning causes reorganization of neuronal firing patterns to represent related experiences within a hippocampal schema," *The Journal of Neuroscience*, vol. 33, no. 25, pp. 10243–10256, June 2013, PMID: 23785140.
- [11] Julien Doyon, Virginia Penhune, and Leslie G Ungerleider, "Distinct contribution of the cortico-striatal and cortico-cerebellar systems to motor skill learning," *Neuropsychologia*, vol. 41, no. 3, pp. 252–262, 2003.
- [12] Laura M Rowland, Reza Shadmehr, Dwight Kravitz, and Henry H Holcomb, "Sequential neural changes during motor learning in schizophrenia," *Psychiatry research*, vol. 163, no. 1, pp. 1–12, May 2008, PMID: 18407471 PMID: PMC2562703.
- [13] Michael E. Tipping, "Sparse bayesian learning and the relevance vector machine," *J. Mach. Learn. Res.*, vol. 1, pp. 211–244, Sept. 2001.
- [14] Jason Weston, Olivier Chapelle, Andr Elisseeff, Bernhard Scholkopf, and Vladimir Vapnik, "Kernel dependency estimation," in *NIPS*, Suzanna Becker, Sebastian Thrun, and Klaus Obermayer, Eds. 2002, pp. 873–880, MIT Press.
- [15] V.A. Tadipatri, A.H. Tewfik, J. Ashe, and G. Pellizzer, "Robust movement direction decoders from local field potentials using spatio-temporal qualitative patterns," in *Engineering in Medicine and Biology Society (EMBC), 2012 Annual International Conference of the IEEE*, 2012, pp. 4623–4626.